ELSEVIER

Journal of Power Sources 63 (1996) 255–266

JOURNAL OF POWER SOURCES

Quantitative modeling of factors determining Ragone plots for batteries and electrochemical capacitors

W.G. Pell, B.E. Conway *

Chemistry Department, University of Ottawa, 10 Marie Curie Street, Ottawa, Ont., K1N 6N5, Canada

Received 7 June 1996; revised 11 October 1996

Abstract

Ragone plots relating power-density to achievable energy-density have been used for many years as an empirical basis for comparative performance evaluation of various battery systems. However, their theoretical basis, and the relative contributions of ohmic and activation (Tafel) polarization effects to the dependence of energy-density on operating power-density have been little studied. Quantitative modeling calculations for various selected values of ohmic resistance, and Tafel exchange-current densities and polarization slopes, *b*, provide rationalizations for the shape of Ragone diagrams and their positions in the log–log plane of energy-density versus power-density plots. Separate evaluations of the ohmic and Tafel polarization 'components' of the Ragone relations are of practical value in the evaluation of the battery performance. The Tafel value *b* is of special importance. Complications which arise in trying to represent electrochemical capacitor behaviour in terms of Ragone-type plots are analysed; they are important for the design and operation of hybrid capacitor/battery systems for electric-vehicle drive trains.

Keywords: Power-density; Energy-density; Batteries; Electrochemical capacitors

1. Introduction

During the past thirty years relations between specific power-density (PD, W kg^{-1}) and energy-density (ED, Wh kg^{-1}) have been empirically plotted, often on logarithmic scales. Such plots originated in an historically significant paper by Ragone [1] at the May 1968 meeting of the Society of Automotive Engineers at Detroit, MI, where the first examples were shown. We specially mention this since Ragone plots are often found in battery literature but the original attribution is rarely quoted nor are interpretations of the plots usually given. In Ragone's paper, the behaviour of battery systems for electrically powered vehicles was already considered, and is now a matter of major importance.

Ragone plots for batteries are now complemented by those for electrochemical capacitors [2,3] especially as the latter are perceived as energy-storage systems capable of high power delivery and high power-level recharging. Of special importance is the hybrid combination of a high-power electrochemical capacitor with a high ED and high charge-capacity battery [4]. Hence the PD and the ED components of the performance of hybrid systems are important to have quantitatively evaluated in order for suitable matching to be achieved and understood on a fundamental basis.

Ragone plots usually have a hooked shape corresponding to a fall-off of ED as PD (i.e. power drain) is increased in discharge of the battery. A theoretical basis for this shape was not provided in Ragone's paper [1] but the general origin of it was recognized qualitatively [1] in terms of increasing cell polarization (hence diminution of cell voltage which determines ED) as higher power demands are made on a battery or capacitor at higher rates of discharge.

A comparison between Ragone plots for advanced electrochemical capacitors and Ni/Cd and lead/acid batteries (specifications not given) was made by Idaho National Engineering Laboratory (INEL, 9-95), by Murphy et al. [3], based on 1995-data, see Fig. 1. Quite high ED in the 7–8 Wh kg^{-1} range for 3 V non-aqueous solvent carbon double-layer-type capacitors and about 1–2 Wh kg^{-1} for 1 V aqueous capacitors are attainable. Pinnacle Research Institute capacitors (probably of the RuO_2 mixed oxide type) provide about 0.4 Wh kg^{-1} at about 400 W kg^{-1}. The 3 V organic electrolyte solution capacitors provide PD'S between 200 W and 3 kW kg^{-1}. The US Department of Energy projected goal is about 1.7 kW kg^{-1}. Such PD levels are observed notwithstanding the intrinsic problem with high-area double-layer capacitors of distributed internal pore resistance [5,6] within

* Corresponding author.

PII S0378-7753(96)02525-6

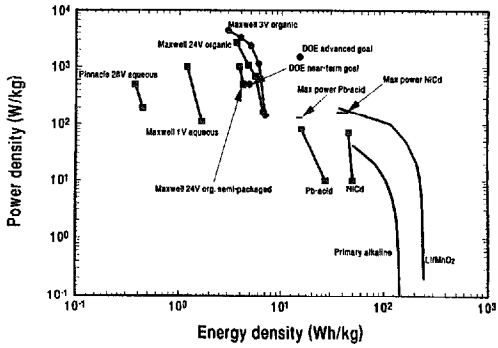

Fig. 1. Ragone plot for ultracapacitors and batteries adapted from Ref. [1,3].

the electrode matrices and a consequent range of resistance–capacitance (RC) time constants leading to non-uniform power capability.

2. Theory

2.1. Formal energy-density and power-density definitions

Energy and power of an electrochemical power source are defined by

$$\text{Energy } (E) = Q(\Delta V), \text{ for a battery} \quad (1a)$$

or

$$\text{Energy } (E) = \frac{1}{2} Q(\Delta V) = \frac{1}{2} C(\Delta V)^2 \text{ for a capacitor} \quad (1b)$$

and

$$\text{Power } (P) = I(\Delta V) \quad (2)$$

where ΔV is the voltage established between the electrodes of a cell, and Q is the charge stored at the potential difference, ΔV. If Q is expressed per unit weight then E is the ED, or if Q is expressed per unit volume, E is the volume ED. In Eq. (2); I is the current drawn on discharge. In practice, the withdrawable charge is usually diminished at elevated power drains due to non-uniformity of discharge and/or isolation of some of the active material at high I values.

From Eqs. (1) and (2) the ratio of energy to power drawn at a given ΔV for a battery is Q/I, and for a capacitor is $Q/2I$, both of which have units of time.

P can also been expressed in terms of the current density, i, defined by $i = I/A$, where A is the accessible surface area of a given electrode. In practice, most battery or capacitor electrodes are three-dimensional porous structures whose A values are usually not precisely known. Then, it is useful to express the current density as a current per unit weight (or volume) of the active materials, which gives immediately the PD per kg or l. We also use the symbol i for this current density.

For a battery system Q is determined, in an elementary way, by Faraday's laws according to the weight, W, of the active material and the number of electrons, z, per mole involved in its oxidation or reduction and, thus, its equivalent weight, M/z, where M is its molar weight. Thus, for a sample weight W

$$Q = FW/(M/z) = zFW/M \quad (3)$$

where F is the Faraday constant, 96 487 C mol^{-1}.

2.2. Dependence of energy-density and power-density on current drain for a battery

Both ED and PD of a battery are determined by the available operating voltage, ΔV, in Eqs. (1a) and (2), respectively. Upon discharge at i, ΔV is diminished jointly by the ohmic polarization iR and the kinetic or activation (Tafel) polarization $\eta_a = a + b \ln i$. R is the ohmic resistance of the electrolyte solution combined with that of the electrode structures.

The Tafel polarization can also be expressed in terms of the exchange current density, i_0, passing reversibly at $\eta_a = 0$ [7]

$$i(\eta_a) = i_0 \exp[\eta_a/b] \quad (4)$$

or

$$\ln i(\eta_a) = \ln i_0 + \eta_a/b \quad (5)$$

where b is the so-called Tafel slope $\mathrm{d}\eta_a/\mathrm{d} \ln i$, also defined as $b = RT/\alpha F$ where α is the transfer coefficient equal to 0.5 ± 0.05 V for most simple, one-electron processes [7].

If there were no polarization losses, obviously, from the above definition of power in Eq. (2), power would increase linearly with i. Since, however, decreases of the thermodynamically available (reversible) potentials at the cell elec-

trodes arise as i increases, and ohmic iR losses arise simultaneously, the power must be expressed as

$$\text{Power } (P) = i(\Delta V) = i[\Delta V_{rev} - iR - \Sigma[\eta_a(i)]] = i\Delta V_{rev} - i^2R - i\Sigma b \ln i + i\Sigma b \ln i_0 \quad (6)$$

where ΔV_{rev} is the reversible cell voltage, b's are for the respective anode and cathode reactions and i_0's have been introduced from Eqs. (4) or (5). Eq. (6) involves the transcendental functions $b \ln i$ and $i\ b \ln i_0$, together with the linear terms in i, and hence can only be numerically solved.

Since RT/i_0F corresponds to a faradaic reaction resistance R_F [7], $i_0 = RT/R_FF$, P can also be expressed in terms of R_F

$$P = i(\Delta V_{rev} - iR - b \ln[R_FF/RT] - b \ln i) \quad (7)$$

where $1/R_F$ measures the kinetic reversibility of the reaction and can be directly determined by means of impedance spectroscopy or from linear polarization slopes for η_a evaluated near the reversible potential [7].

In Eq. (6) $i\Delta V_{rev}$ is the ideal power available with increasing i; if ΔV_{rev} were uninfluenced by the magnitude of i, P would increase linearly with i. This is actually observed for sufficiently low i values that the ohmic and Tafel polarizations remain small. From Eq. (6) it is clear that although P will initially tend to increase with current drain i, it must eventually decrease due to the negative terms in ohmic and kinetic polarizations. Hence there is a maximum in power withdrawable from a cell with increasing i determined by differentiating P with respect to i; thus

$$dP/di = \Delta V_{rev} - 2iR - (i)\Sigma b/i - \Sigma b \ln(i) + \Sigma b \ln(i_0) \quad (8)$$

$$= \Delta V_{rev} - 2iR - \Sigma b - \Sigma b \ln(i) + \Sigma b \ln(i_0) \quad (9)$$

$$= 0 \quad \text{for the maximum in } P$$

The P_{max} arises at a current determined by the transcendental equation

$$2iR + \Sigma b \ln i = \Delta V_{rev} + \Sigma b \ln i_0 - \Sigma b \quad (10)$$

for which no explicit solution is possible so that the i at which P_{max} arises must be determined numerically.

Note that P_{max} is determined both by i and $\ln i$; thus, with increasing i, it is seen that the rate of decrease of P is actually mainly determined by the ohmic iR term which is therefore practically a more important factor than the kinetic polarization at high i unless R is relatively negligible. However, there is additionally the 'constant' factor, Σb, related to sums of the Tafel slopes for anodic and cathodic half-cell reactions of the cell. Also, of course, better maximum power is attained when the reversible cell voltage, ΔV_{rev}, is larger, i.e. for a bigger open-circuit e.m.f. or 'driving force' of the cell.

Correspondingly, a maximum in $\ln P$ arises in the ln–ln Ragone plot when $d \ln P/d \ln E = 0$. Thus with

$$\frac{d \ln P}{d \ln E} \equiv \left(\frac{E}{P}\right)\frac{dP}{dE} = 0 \quad (11)$$

and with

$$V = E/Q = \Delta V_{rev} - iR - \Sigma(a + b \ln i)$$

$$\frac{d \ln P}{d \ln E} = \frac{E}{P}\frac{V - iR - \Sigma b}{Q/i(-iR - \Sigma b)} = \frac{E}{Q(-iR - \Sigma b)} + 1 = \frac{V}{-iR - \Sigma b} + 1 = 0 \quad (12)$$

From Eq. (12), PD increases with ED for the conditions

$$\frac{d \ln P}{d \ln E} > 0 \text{ for } V < iR + \Sigma b \quad (13a)$$

while it decreases with increasing ED for

$$\frac{d \ln P}{d \ln E} < 0 \text{ for } V > iR + \Sigma b \quad (13b)$$

and the maximum in PD with respect to ED occurs when

$$V = iR + \Sigma b \quad (14)$$

i.e. V for P_{max} increases with R and b values but P itself decreases.

Note that at sufficiently high power drain (virtually a short-circuit), V will be reduced to zero so that $iV = V = 0$ which arises when

$$i(\Delta V_{rev}) = i^2R + i\Sigma b \ln i - i\Sigma b \ln i_0 \quad (15)$$

or

$$\Delta V_{rev} = iR + \Sigma b \ln i - \Sigma b \ln i_0 \quad (16)$$

i.e.

$$\Delta V_{rev} = iR + \eta_a(i) \quad (17)$$

Practically, this arises when i tends to be sufficiently large that the iR drop virtually completely opposes the ΔV_{rev} so that no useful power is any more available.

The ED (Eq. (1)) also, of course, depends on the diminution of ΔV_{rev} due to the same polarization effects that influence P; thus

$$E = Q(\Delta V_{rev} - iR - \Sigma b \ln i + \Sigma b \ln i_0) \quad (18)$$

cf. Eq. (6), where the term in brackets, equal to E/Q is identical with the term P/I of Eq. (6).

It is the relation between E in Eq. (18) and P in Eq. (6) that is the basis of Ragone plots for battery systems.

An additional factor can sometimes be the concentration polarization in certain cells, e.g. with soluble redox reagents or fuel cells with soluble fuel, e.g. CH_3OH. That is, at sufficiently high current drains, $i \approx i_l$, power becomes limited by mass transport of the reagent or limiting by zero concentration of the reagent at the reactive electrode surface.

Concentration polarization, η_c, is defined by the equation

$$\eta_c = \frac{RT}{F} \ln\left[\frac{i_l}{i_l - i}\right] \quad (19)$$

Here, i_l is the limiting current that arises when the concentration of the reactive species at the electrode surface is reduced to zero corresponding to maximized concentration gradient at the electrode surface. In this case, the cell potential varies as

$$V = \Delta V_{rev} - iR - \Sigma(\eta_a) - \Sigma(\eta_c) \quad (20)$$

where η_a is the activation polarization and η_c is the concentration polarization.

2.3. Ragone plots for electrochemical capacitor behaviour

Ragone plots have taken on a new importance in the technology of combination of electrochemical capacitors having high PD (but relatively low ED) with high ED aqueous electrolyte batteries for electric-vehicle drive trains [4]. For such systems power level and energy balancing in the coupling between these two kinds of energy-storage systems is of major importance [4] and consequently requires quantitative knowledge of the Ragone relations for both types of system.

As we show below, the factors that determine the ED versus PD relations for electrochemical capacitors are significantly different from those for batteries because, on discharge, a continuous decline of output voltage is an intrinsic property of a charged capacitor (determined by the relation $C = Q/V$) while, ideally, a battery discharge voltage can remain constant so long as the chemical redox species remain in a two-phase electrochemical equilibrium prior to exhaustion of one or other of the reactants, as is well exemplified by the case of discharge of Li/$SOCl_2$ primary batteries. Practically, of course, most secondary batteries do show to some, often significant degree, a decline of cell voltage upon discharge (e.g. with Li intercalation systems, see Ref. [8]), and this has to be taken into account in the evaluation of battery/capacitor hybrid-power systems.

We now examine how rating of PD of a capacitor can be treated and experimentally examined.

Formally, there is an important difference between the principle involved in rating power drain from an ideal battery and that applicable to capacitors, defining an ideal battery as one for which the cell voltage through the discharge half-cycle remains almost constant. As emphasized earlier, an essential feature of the electrical behaviour of a capacitor is a decline of voltage upon discharge in proportion (when its capacitance is independent of potential difference between its 'plates') to charge removed through an external load, i.e. $V = Q/C$ or $dV/dQ = C^{-1}$. Hence, withdrawal of charge at a rate i causes a corresponding rate of decline in V so that a formal power rating at a particular i depends on the state of discharge of the capacitor.

With the usual definition of PD as iV we have

$$P = i(Q/C) \text{ or, differentially } P = VC(dV/dt) \quad (21)$$

for a given constant discharge $i(= dQ/dt = C\ dV/dt)$ and, for C invariant with potential, dV/dt = constant for a given fixed i.

In another way, we can write the charge remaining on the capacitor at time t, beyond some initial condition (i) when the charge was Q_i, as

$$Q_t = Q_i - \int i\,dt \quad (22)$$

The corresponding potential V_t is Q_t/C, i.e.

$$V_t = (Q_t - \int i\,dt)/C \quad (23)$$

so that the PD at time t, after commencement of discharge at i A cm^{-2}, will be

$$P_t = i(Q_i - \int_0^t i\,dt)/C \quad (24)$$

The initial PD (P_i) was iV_i or iQ_i/C so that

$$P_t = iV_i - i\int_0^t i\,dt/C \quad (25)$$

$$= i(V_i - \int_0^t i\,dt/C) \quad (26)$$

which eventually, of course, becomes zero when

$$\int_0^t i\,dt/C = Q_i/C = V_i$$

Alternatively, a capacitor device could be discharged under conditions of constant power, iV = constant. For such a situation, as charge was being withdrawn and V declining, it would be necessary to arrange instrumentally that i would be increasing in order to maintain the product iV = constant, $= k$ say. In fact, $i = kV^{-1}$ so that the condition

$$di/dV = -kV^{-2} \quad (27)$$

would be required. $V(= V_t)$ at any time t during this constant power discharge would be $V_t = Q_t/C$ in terms of the charge Q_t remaining at time t into the discharge. Hence

$$di/dV = -k/(Q_t/C)^2 \quad (28)$$

i.e. i must increase as V decreases, which is the basis of this case.

These relations show that PD evaluation for a capacitor is not as simple as for an ideal battery.

Additionally, as for a battery, the PD will decline (at a given degree of charge Q_t held by the capacitor) with increasing discharge rate i when there are ohmic polarization losses.

This will certainly be the case with porous, high-area capacitor electrodes, especially when less conductive non-aqueous electrolytes are employed as in the case of the higher operating voltage double-layer capacitors. Note that for capacitors, there are normally no kinetic Tafel polarization losses involved in the PD evaluation. However, for electrochemical capacitors utilizing redox or adsorption pseudocapacitance [9], additional faradaic (Tafel-type) polarization losses will arise, as was discussed earlier for the case of PD versus ED Ragone plots for batteries.

As with battery systems, the rated PD of capacitors will depend on the current drain at which the rating is evaluated; it will also depend on the state-of-charge (SOC) in the capacitor case much more than for most battery systems except for the case of Li intercalation types where quasi- or pseudocapacitor behaviour can arise [8].

A final difference between capacitor- and battery-power rating is the relation between PD and ED for these two types of electrical energy storage system. Eqs. (1) and (2) show that there is an essentially direct relation between PD (iV) and ED (QV or $0.5QV$) for a given initial cell voltage since, for both cases, the factor by which the cell voltage is diminished by polarization effects with increasing i is, at least theoretically, the same. However, in the case of capacitors, the density of stored energy scales with the square of the voltage attained at the end of charge while the PD remains linear in that voltage, though for both properties the voltage can be controllably raised (unlike for the case of the thermodynamic voltage of most battery cells) up to, or just below, the electrolyte solution decomposition potential limit (i.e. about 1.3 V for aqueous solutions or about 3.5–4.0 V for a non-aqueous aprotic solvent solutions). The above statement implies the interesting conclusion that the ratio of ED to PD for a given capacitor is a function of potential on charge, i.e. this ratio increases towards completion of charging which is not normally the case for ideal battery cells.

A maximum in PD with respect to ED at a particular SOC defined by an open-circuit potential V_i is also predicted theoretically for capacitors. Given that for a particular SOC of a capacitor

$$V = V_i - iR$$

on discharge

$$P = i(V) = iV_i - i^2R$$

and

$$E = \frac{1}{2}CV^2 = \frac{C}{2}(V_i - iR)^2$$

the slope of the ln–ln Ragone relation is, therefore

$$\frac{\mathrm{d}\ln P}{\mathrm{d}\ln E} = \frac{E\,\mathrm{d}P/\mathrm{d}i}{P\,\mathrm{d}E/\mathrm{d}i} = \frac{1/2CV^2(V_i - 2iR)}{iV(-CRV)} = 0$$

$$= \frac{V_i}{-2iR} + 1 = 0 \qquad (29)$$

The ED corresponding to the maximum PD, viz. $P_{max} = V_i^2/4R$ [10], corresponding to the conditions given by Eq. (29), is then

$$E_{\text{at } P_{max}} = \frac{CV_i^2}{8}$$

3. Results and discussion

3.1. Quantitative evaluations of polarization effects in battery discharge

In Section 2.2 we have given equations which represent the effects of (i) ohmic (iR) polarization and (ii) kinetic (Tafel) polarization on both the ED and the PD of battery systems on discharge which characterize the Ragone plot for a given system. Here we show by means of some quantitative numerical calculations how the following parameters of battery systems determine the shape and position of Ragone plots between the scales of ED and PD. Both these quantities depend (cf. Eqs. (6) and (18)) on the electric polarizations suffered at the battery electrodes which increase logarithmically with i in the kinetic (Tafel) regime and linearly in i in the ohmic (iR) regime. Normally both factors have to be considered except at extremes of discharge-current values.

The parameters are (i) the internal ohmic resistance, R, of the battery system (electrolyte and electrode structures) and (ii) the Tafel equation parameters a (or i_0) and b characterizing the dependence of η_a on ln i. Both the R and the Tafel parameters have been recognized qualitatively as determining factors in Ragone plots [11], e.g. for fuel-cell performance [11], but quantitative numerical evaluations for battery systems have been lacking, especially the separate roles of the values of the Tafel slopes for the anode and cathode reactions. Ragone plots themselves are usually shown on an empirical basis with little or no reference to the relative importance of the ohmic and kinetic contributions to the PD versus ED relations. It is the aim of the 'theoretical' calculations, the results of which are shown diagrammatically in the figures below, to demonstrate the relative influences of the ohmic and kinetic effects for arbitrary but realistic selections of parameter values. Although the parameters we have chosen to represent Ragone plots for various conditions are arbitrary, they have been selected to correspond to ranges of practical behaviour commonly observed. In the case of the ohmic polarization factor, which diminishes cell voltage and hence both PD and ED, it is to be noted that $i \times R$ scale together so that the equivalent behaviour arises, for example, with high i and low R as for low i and high R. The important factor determining the shape and position of Ragone plots in the PD versus ED plane is how the iR polarization compares with increasing Tafel polarization as i is increased with increasing operating power, see Eqs. (6) or (7). Also, the separate dependences of the ED and PD on i are useful to evaluate in relation to corresponding Ragone plots.

The following are the bases of the calculations for simulated Ragone plots for batteries:

(i) An overall polarization equation for electrode potential V as a function of i (including iR and η_a, but excluding η_c) is written (cf. Eq. (6)) as

$$V = \Delta V_{rev} - iR - (a + b \log i) \quad (30)$$

Nominal values of $\Delta V_{rev} = 1$ V and $i_0 = 10^{-5}$ A kg^{-1} are taken. The Tafel constant a is $-b \log i_0$.

(ii) Energy-density, E, is taken as $Q \times V$ where Q is the charge capacity in MC kg^{-1} (about 10 F), nominally taken as 1 for the purpose of calculations of relative behaviours.

(iii) Power-density, P, is taken as $i \times V$.

(iv) V, E and P were calculated for $R = 0.01$, 0.1, 1.0 and 10 Ω, and values of the Tafel parameters a, b, respectively, as 0.6 and 0.120 V, 0.21 and 0.042 V, 0.15 and 0.03 V and limitingly as 0 and 0 V (no kinetic polarization). Other values of a, corresponding to various other selected values of ln i_0, could, of course, be taken.

The calculations resulted in a family of 16 log P versus log E curves; the range of i values for each curve was selected such that $V > 0$, i.e. $P > 0$, $E > 0$, and that the curves covered the range of i values within which the expected maximum in P (Eq. (10)) would be demonstrated. Note that Eq. (30) predicts (when multiplied by i) an initial increase in P with increasing i when i is sufficiently small that the two polarization terms which diminish V from ΔV_{rev} are negligible but a decrease in P at larger i values; hence a maximum in P arises, as was shown analytically in Eqs. (9), (10) and (12). However, it is interesting that almost all empirically determined Ragone plots (e.g. Fig. 1) do not exhibit maxima but only a roll-off of P with increasing i and hence diminishing E. This is presumably because, with practical systems, sufficiently high discharge currents were not used in the performance tests to reach and exceed the maximum in P, or alternatively current limitation by diffusion control had set in, as may arise in fuel cells and some batteries, e.g. due to consumption of Li^+ ions or to pH changes.

The following summarizes the set of log P versus log E, and P or E versus log i relations calculated:

(i) Fig. 2(a)–(d), constant b value, various values of $R = 0.01$, 0.1, 1.0, 10.0 Ω;

(ii) Fig. 3(a)–(d), constant R, various values of $b = 0.120$, 0.042, and 0.030 V;

(iii) Fig. 4, constant $b = 0.120$ V, various values of R for P and for E as a function of log i; and

(iv) Fig. 5, $R = 1$ Ω, with various b values for log P and for E versus log i.

It will be useful now to present a commentary, in a comparative way, on the forms of these results as shown in the above figures. In all the computed series of Ragone plots in Figs. 2(a)–(d) and 3(a)–(d), ED at first decreases almost

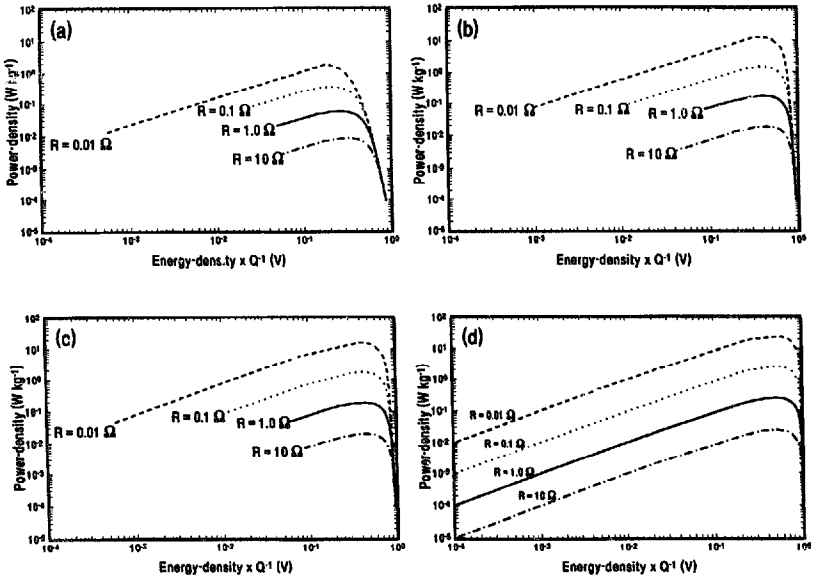

Fig. 2. Calculated Ragone diagrams for a battery having $\Delta V_{rev} = 1$ V, $i_0 = 10^{-5}$ A kg^{-1}, showing the effect of ohmic polarization for fixed Tafel polarization: (a) $b = 0.120$ V, $a = 0.60$ V; (b) $b = 0.042$ V, $a = 0.21$ V; (c) $b = 0.030$ V, $c = 0.15$ V; (d) $b = 0$ V, $a = 0$ V.

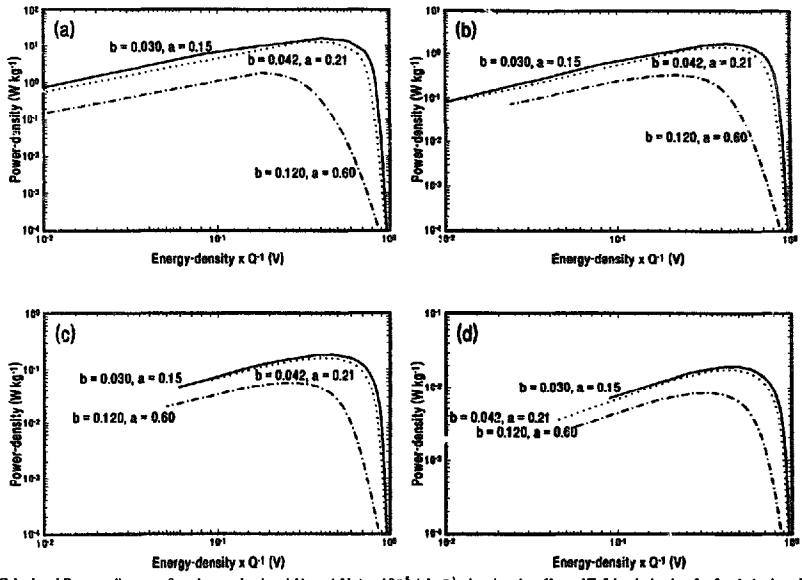

Fig. 3. Calculated Ragone diagrams for a battery having $\Delta V_{rev} = 1$ V, $i_0 = 10^{-5}$ A kg^{-1}, showing the effect of Tafel polarization for fixed ohmic polarization: (a) $R = 0.01\ \Omega$; (b) $R = 0.10\ \Omega$; (c) $R = 1.0\ \Omega$, and (d) $R = 10.0\ \Omega$.

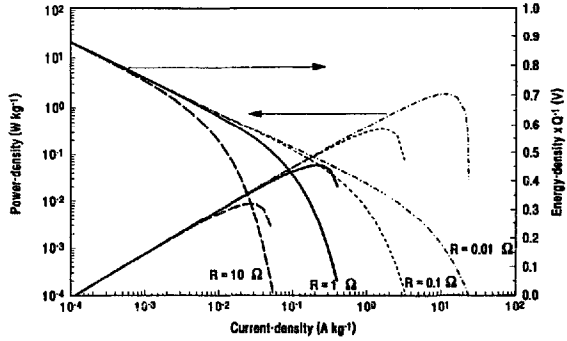

Fig. 4. The effect of ohmic polarization on PD and reduced ED as a function of i for a battery characterized by $\Delta V_{rev} = 1$ V, $i_0 = 10^{-5}$ A kg^{-1}, $b = 0.120$ V, and $a = 0.60$ V.

linearly with increasing PD (on the log–log plots) in the first decade of values of ED 0.1 to 1 Wh kg^{-1}. Then the PD maximum (Eqs. (9), (10) and (12)) is attained followed by progressively decreasing PD with decreasing ED, the PD levels attained being progressively lower (as expected) for the larger R values (greater iR-drop component values). The slopes of the log P versus log E lines below the P_{max} are approximately the same for small i and, as $i \rightarrow 0$ approach 1 (as expected according to Eq. (12)). The roll-off, before the maximum power is attained, takes place at lower power as R is increased from 0.01 to 10 Ω or more as, is intuitively expected.

Fig. 2(a) is calculated for $b = 0.120$ V, $a = 0.6$, Fig. 2(b) for $b = 0.042$ V, $a = 0.21$, Fig. 2(c) for $b = 0.029$ V, $a = 0.15$ and Fig. 2(d) (reference case), for $b = 0$, $a = 0$ (zero kinetic polarization). Fig. 2(d) thus illustrates the limiting case

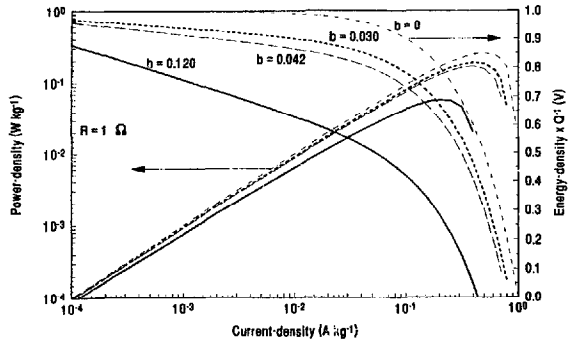

Fig. 5. The effect of Tafel polarization on PD and reduced ED as a function of i for a battery characterized by $\Delta V_{rev} = 1$ V, $i_0 = 10^{-5}$ A kg-1, and $R = 1$ Ω.

where only iR polarization determines the shape of the Ragone plots. The power, is of course, attenuated as R is increased from 0.01 to 10 Ω, or more.

The b values were chosen as those typically considered and often observed for the hydrogen-evolution reaction and other well-known electrode processes [7,12].

The series of Fig. 3(a)–(d) shows Ragone plots resulting from variation of Tafel slope b values with a selected fixed R value taking $R = 0.01$, 0.1, 1.0 and 10 Ω each for a series of three b values.

The same general forms of the resulting Ragone plots in the series '3' calculations arise as in the series '2' but the variation of b mainly affects the shape of the Ragone plot at the high ED (low i) end before the maximum in P arises (with decreasing E). The curves again have the same slopes (parallel lines) beyond the maxima, at decreasing E values, almost independently of the assigned Tafel slope value. Again, the power levels attained diminish with increasing values of the chosen R, 0.01 to 10 Ω. It is the high ED ends of the Ragone plots that are most affected by the assigned b value, i.e. where the kinetic polarization increases with increasing i the more rapidly the greater is the b value in the series $b = 0.029 < 0.042 < 0.120$ V.

3.2. Individual dependences of P and E on log i

In the evaluation of battery power systems, the Ragone relations are not usually expressed complementarily in terms of the individual P and E values as a function of i. However, this is an informative way of examining the data for a given power source. Using the quantities calculated for Figs. 2 and 3, Figs. 4 and 5 show the dependences of both P and the reduced ED (E/Q) on log i for variation of R from 0.01 to 10 Ω, for $b = 0.120$ V ($V_i = 1.0$ V) (Fig. 5) and in Fig. 6 for variation of b taken as 0.029, 0.042, 0.120 V with a single value for R, taken as 1 Ω. These show clearly how the PD falls off, after the maximum, only strongly at high i in the decade 0.1 to 1 A kg^{-1}. There is a broader fall-off of E/Q both with increasing R (0.01 to 10 Ω, Fig. 5) and increasing b (Fig. 6). The plots for ED versus log i for increasing R closely resemble the form of Tafel relations for a given a (or log i_0) and b value with increasing solution resistance in series with the electrode.

Finally, in this analysis of the relation between effects of iR and η_a polarization, it is informative to show the progressive changes of the form of a 'Tafel' plot with increasing iR-drop component in the overall $iR + \eta_a$ polarization. This can be done in a generalized way by plotting reduced current density as i/i_0 on the axis of abscissae against a polarization quantity $\eta = \eta_a + iR$ with iR taken as $i_0R \times i/i_0$ for a series of values of R expressed as $i_0R = 0$ to $i_0R = 2 \times 10^{-2}$, as shown in Fig. 6. Here the transition from pure Tafel (logarithmic) polarization behaviour (curved on the linear plot versus i/i_0 with $i_0R = 0$) to much more linear behaviour (on the linear

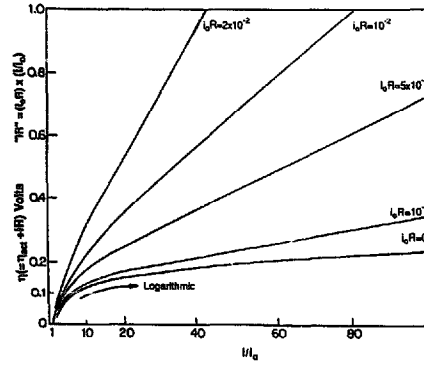

Fig. 6. Effect of combination of a linear (ohmic) and exponential (Tafel) polarization effect on generalized current vs. potential curves for an electrode process. Current-density scale: relative i/i_0; overpotential scale: $\eta + iR$ ($iR = i_0R \times i/i_0$). Diagram shows transition from mainly 'Tafel' to mainly 'ohmic' polarization for a Tafel slope of 0.118 V and $i = i_0 \times 10^{\eta/b}$.

i/i_0 plot) is seen with increasing values of the i_0R polarization component.

3.3. Ohmic and Tafel polarization components of Ragone plots

It is interesting and useful, for comparative practical evaluation of electrochemical power sources, to evaluate and thus distinguish separately the ohmic and the Tafel polarization components that determine the form of Ragone plots.

In Fig. 7 are plotted reduced EDs, i.e. E/Q, a quantity in V, against log i. Fig. 7 shows the components of this voltage for a given Tafel slope ($b = 0.120$ V) and a variable iR component with R varying from 0.01 to 10 Ω, line A shows the reduced ED prior to polarization corrections, line B represents the ED losses due to Tafel polarization, lines C1, C2, C3 and C4 the ED losses due to ohmic effects, and lines E1, E2, E3 and E4 the net ED of the systems. This figure can be analysed to determine the i range over which each of the polarization terms dominates the behaviour of the resultant ED. At low i, the ED is linear in log i, and clearly, the Tafel polarization component, which is much larger than the iR component in this region, is dominant. For a fixed Tafel slope, and variable R, the current range over which the ED versus log i curve is linear, increases as R decreases. At high current densities, the iR polarization increases rapidly (cf. Fig. 7) relative to the Tafel polarization component and results in a sharp decline in the ED. A similar analysis of E/Q for fixed R and varied b shows that a larger value of b leads to a greater component of kinetic polarization for a given value of i, other things being equal. Thus, the diminution of ED can be quite significant for large b even at small i. This component analysis shows that η_a is most important at high ED (low i) rather than at high PD (higher i).

Fig. 8 shows plots of the contributions of ΔV_{rev}, iR and $(a + b \log i)$ to the PD. Each of the terms in Eq. (6), $i\Delta V_{rev}$, i^2R and $i(a + b \log i)$ were calculated for specific parameter values (R, a, and b) and are plotted versus log i. The curves in Fig. 8 are for a fixed iR component ($R = 1.0$ Ω) and a varied Tafel slope, $b = 0.120$, 0.029, 0 V and have been plotted as a linear log relation, as for the E/Q diagram, line A is the polarization-free PD, B the iR polarization contribution, C1 and C2, the η_a components; P1, P2, and P3 are the polarization-corrected PD's.

The interpretation of these figures is more difficult than for the complementary ED diagrams previously discussed for which the reduced ED, before correction for polarization losses, was constant for all i's (Fig. 7, line A = 1). The PD before correction for polarization losses, is, of course, directly dependent on i as defined by $i \times \Delta V_{rev}$. Furthermore, neither the decrease in PD due to η_a nor to iR is linear in log i.

Several general statements regarding these diagrams can be made: again, as for the case of ED, the activation polarization is of greater significance at low i, and the iR contribution is larger at high i. Interestingly, it is only when both $i\eta_a$ and i^2R are significant with respect to $i\Delta V_{rev}$ that maxima in the PD curves arise.

At sufficiently low i, ED is significantly reduced as i increases (Fig. 7) and is controlled by η_a, whereas PD is relatively independent of i (Fig. 8) and is relatively small. At intermediate i, ED decreases more rapidly as both iR and η_a reduce the operating voltage, (Fig. 7). Power density increases as the $i\Delta V_{rev}$ term dominates the i^2R and $i\eta_a$ polarizations. At high i, ED drops sharply towards zero and PD reaches a maximum and then decreases. Energy-density decreases over the full range of i, whereas the change in PD is significant only at intermediate and high i values.

3.4. Discussion of calculations for power-density versus energy-density of a capacitor

The following are the bases of the calculations for simulation of Ragone plots for capacitors:

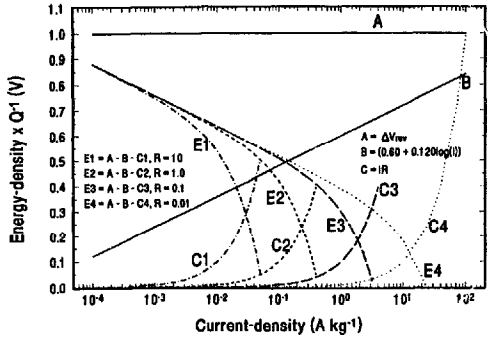

Fig. 7. Contribution of ohmic and Tafel polarization to reduced ED as a function of i for a battery characterized by $\Delta V_{rev} = 1$ V, $i_0 = 10^{-5}$ A kg^{-1}, $b = 0.120$ V, and $a = 0.60$ V. Line A corresponds to the ED of a battery prior to polarization corrections, line B represents ED losses due to Tafel polarization, lines C1, C2, C3 and C4 to ED losses due to ohmic effects for $R = 10$, 1.0, 0.1, and 0.01 Ω, respectively and lines E1, E2, E3 and E4 the net ED of the systems.

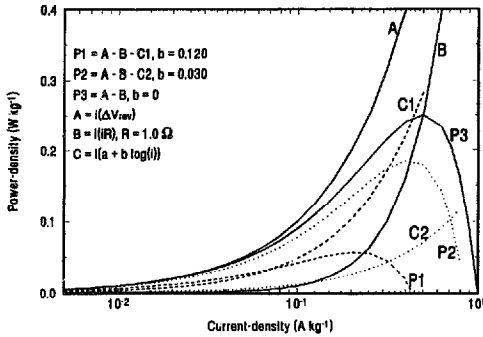

Fig. 8. Contributions of ohmic and Tafel polarization to PD as a function of i for a battery characterized by $\Delta V_{rev} = 1$ V, $i_0 = 10^{-5}$ A kg^{-1}, $R = 1.0$ Ω. Line A corresponds to the PD of a battery prior to polarization corrections, line B represents PD losses due to ohmic polarization, lines C1 and C2 to PD losses due to Tafel effects for $b = 0.120$ and 0.030 V, respectively, lines P1, P2 and P3 the net PD of the systems.

(i) An overall polarization equation for electrode potential as a function of i is taken as $V = V_i - iR$.

b) Energy-density, E, is taken as $1/2QV = 1/2CV^2$, where Q is the charge capacity in MC kg^{-1}, nominally taken as 1 MC kg^{-1} (about 10 F).

(iii) Power-density, P, is taken as $i \times V$.

Fig. 9 illustrates the Ragone plots for fully charged capacitors having constant Q (= 1 MC kg^{-1}), and variable nominal C (= 2.0, 1.0, 0.5 and 0.1 MF kg^{-1}) values. Each of these cases defines an initial open-circuit potential for a charged capacitor of V_i (= 0.5, 1, 2, and 10 V). The effect of iR polarization is included in this analysis for $R = 0.1$, 1.0 and 10 mΩ. As discussed by Miller [10], a capacitor is considered effectively discharged when the operating potential falls to $V_i/2$, at which time the capacitor has delivered 75% of its charge capacity into a load resistance. For a constant-load discharge, the remaining 25% of capacity can only be recovered over an extended time and increasingly lower i (remembering that current decreases exponentially in time through a constant resistance load). Thus the curves in Fig. 9 correspond to potentials between V_i and $V_i/2$. Decreasing C while maintaining Q constant, increases the initial operating voltage and thus both the maximum ED and PD attainable. If the capacitor is discharged past $V_i/2$, both ED and PD will decrease, cf. Eq. (29). Obviously, decreasing the iR polarization increases the maximum PD. The maximum ED is effectively independent of R, as it always arises when $i \to 0$.

Fig. 10 shows how the SOC dependence of ED and PD values can be calculated as a function of i. Here Q_i (Eq. (22)) is taken as 1 MC kg^{-1}, C as 1 MF kg^{-1}, V_i as 1 V and R as 10 mΩ. The resulting ED/PD relationships were calculated as a function of i for a capacitor holding 56, 36 and 25% of the charge capacity (on an Ah basis) of the fully charged capacitor. Clearly (see Fig. 10) both ED and PD are dependent on the SOC of the capacitor, and the maximum PD deliverable by the capacitor decreases as the capacitor is

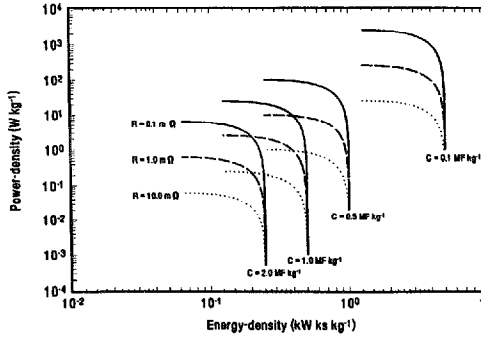

Fig. 9. Calculated Ragone plots for fully charged capacitors having constant $Q = 1$ MC kg^{-1}, variable nominal C (= 2.0, 1.0, 0.5 and 0.1 MF kg^{-1}) values, and variable ohmic polarization ($R = 0.1$, 1.0, 10.0 mΩ).

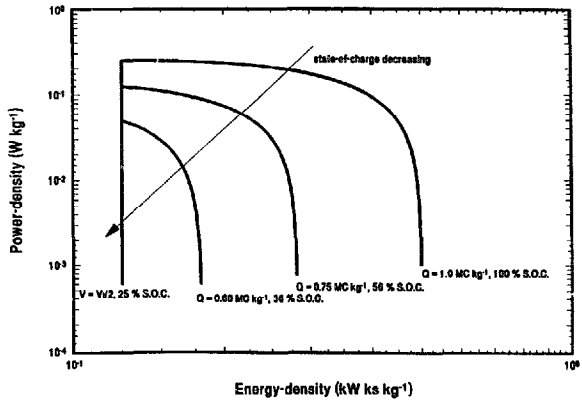

Fig. 10. Calculated Ragone plot showing the SOC dependence of ED and PD for a capacitor characterized by $Q_t = 1$ MC kg^{-1}, C as 1 MF kg^{-1}, $V_i = 1$ V and $R = 10.0$ mΩ holding 100, 56, 36 and 25% of the charge capacity (on Ah basis) of the fully charged capacitor.

discharged. This is a significant practical characteristic that must be considered during system design of battery/capacitor hybrids.

Fig. 11 illustrates normalized ED and PD versus i plotted as a function of the SOC for conditions as described for Fig. 10. Fig. 11 reinforces the significance of the dependence of both ED and PD on the SOC of the capacitor, and illustrates that there is a maximum power point (MPP) of operation and that the MPP is dependent on SOC. The MPP corresponds to the current density and device potential at which maximum power-density may be delivered. In Fig. 11, the dark solid lines correspond to the EDs and PDs up to the cutoff voltage for a discharged capacitor of $V_i/2$; the dashed lines to an ED limit of 0. As the SOC is decreased, the energy limit (viz. 25% of the energy of the fully charged capacitor remaining at the cutoff voltage of $V_i/2$) is reached at progressively lower i's, and clearly this limit is attained at i's smaller than those defined by the MPP. It is, therefore, impossible to operate at the MPP for any SOC other than 100%, illustrating that the choice of the optimum capacitor (i.e. selection of Q, C, V_i) for a particular application is not a simple problem.

3.5. *Kinetic polarization factor in Ragone plots for a pseudocapacitance device*

In Section 3.4 the polarization of the capacitor was assumed to be ohmic ($V = V_i - iR$) due to the internal resistance of the porous electrode matrix and of the electrolyte within it. Such conditions apply principally to the 'double-layer' type of supercapacitor. However, when the charge stor-

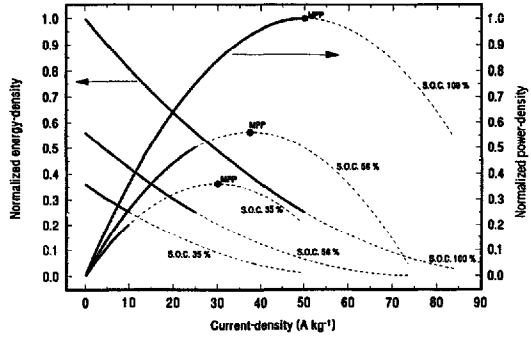

Fig. 11. Normalized ED and PD vs. i plotted as a function of SOC for a capacitor characterized by $Q_t = 1$ MC kg^{-1}, C as 1 MF kg^{-1}, $V_i = 1$ V and $R = 10.0$ mΩ holding 100, 56 and 36% of the charge capacity (on Ah basis) of the fully charged capacitor. Solid lines correspond to the EDs and PDs up to the cutoff voltage for a discharged capacitor of $V_i/2$; the dashed lines to an ED limit of 0.

age of the device originates principally from faradaic pseudo-capacitance (e.g. associated with electrosorption [13] or solid-state or surface redox processes, as with RuO_2 [9]), then the analysis for battery-type polarization relations developed in Section 2.2 will apply, i.e. when both the ohmic and Tafel polarization factors are involved.

However, in the case of a supercapacitor energy-storage device, independently of whether the capacitance arises electrostatically from the interfacial double-layer or faradaically mainly from pseudo-capacitance, the potential will decline with extent of discharge uniformly if the capacitance were constant or in a more complex way if the capacitance itself has some dependence on potential as is often the case experimentally [9,13,14].

This factor of decline in potential with extent of discharge is a general and intrinsic characteristic of any type of capacitor device; it is the main factor which distinguishes the behaviour of batteries from that of capacitors reflected in the qualitative difference between Ragone plots for capacitors and those for batteries, with the exception (cf. Ref. [8]) of the lithium-intercalation type. This difference is illustrated in the present paper through Figs. 9–11 in relation to Ragone plots for battery-type energy storage systems shown earlier.

4. Conclusions: interpretation of practical Ragone diagrams

In Figs. 3 and 4 we showed that the maximum in PD for a battery system defined by an open-circuit potential of V_i, is primarily determined by the iR losses, provided that R is not negligibly small, and that the negative slope of PD versus ED is determined by losses associated with the η_a. A large negative slope indicates a low η_a, and a smaller slope, a high η_a. Obviously, a low η_a and therefore a sharp decrease in PD at high ED is preferred. The maximum in ED arises as $i \rightarrow 0$, where losses associated with η_a are significantly larger than iR losses. Thus, a low η_a also favours a high ED.

From Figs. 8–10 it is seen that the Ragone plot for a fully charged capacitor is effectively at a constant PD over most of the range of ED. Further, and of major practical importance, such a Ragone plot is substantially dependent on the SOC, and, as the capacitor discharges, the log P versus log E dependence becomes more sloping (Fig. 9). Matching of capacitor/battery systems should take into account this dependence of the capacitor PD versus ED relation on SOC. Thus, in an hybrid capacitor load-levelled battery system for electric-vehicle application [3,4], optimal performance of the battery–capacitor combination will be achieved along the initial, almost flat part of the Ragone curves where PD remains almost constant. Obviously also, as seen from Fig. 10, the best power performance provided by the capacitor component will be realized when the system is operated at the highest possible SOC, e.g. maintained by recharge from the battery component on level and uniform-speed driving and/or from a regenerative braking system.

Acknowledgements

Grateful acknowledgment is made to the Natural Sciences and Engineering Research Council for support of this work on a Strategic Grant. We also thank Dr J. Miller of JME Inc. for useful discussions during the course of this work.

References

[1] D. Ragone, *Proc. Soc. Automotive Engineers Conference, Detroit, MI, USA, May 1968.*
[2] J. Miller, in S. Wolsky and N. Marincic (eds.), *Proc. 3rd Int. Symp. Double-Layer Capacitors and Related Devices*, Florida Educational Seminars, Boca Raton, FL, 1993.
[3] T.C. Murphy, G.H. Cole and P.B. Davis, in S. Wolsky and N. Marincic (eds.), *Proc. 5th Int. Symp. Double-Layer Capacitors and Related Devices*, Florida Educational Seminars, Boca Raton, FL, 1995.
[4] A. Burke, in S. Wolsky and N. Marincic (eds.), *Proc. 2nd Int. Symp. Double-Layer Capacitors and Related Devices*, Florida Educational Seminars, Boca Raton, FL, 1992.
[5] J. Miller, in S. Wolsky and N. Marincic (eds.), *Proc. 2nd Int. Symp. Double-Layer Capacitors and Related Devices*, Florida Educational Seminars, Boca Raton, FL, 1992.
[6] R. Levie, *Electrochim. Acta, 8* (1963) 751.
[7] K.J. Vetter, *Electrochemical Kinetics*, Academic Press, New York, 1967, p. 343.
[8] B.E. Conway, *Electrochim. Acta. 38* (1993) 1429.
[9] B.E. Conway, *Proc. Electrochemical Society Symp. Electrochemical Capacitors, Chicago, IL, USA, Oct. 1995*, Prov. Vol. 95-2, The Electrochemical Society, Pennington, NJ, USA, 1996.
[10] J. Miller, in S. Wolsky and N. Marincic (eds.), *Proc. 4th Int. Symp. Double-Layer Capacitors and Related Devices*, Florida Educational Seminars, Boca Raton, FL, 1994.
[11] S. Srinivasan and J.O'M. Bockris, *Fuel Cells: Their Electrochemistry*, McGraw Hill, New York, 1969.
[12] B.E. Conway, *Theory and Principles of Electrode Processes*, Ronald Press, New York, 1964.
[13] B.E. Conway and E. Gileadi, *Trans. Faraday Soc., 58* (1962) 2493.
[14] D.C. Grahame, *Chem. Rev., 41* (1947) 441.